SI MATERIALS AND METHODS

Reagents and antibodies. Phencyclidine **(**PCP) was from Sigma (Ronkonkoma, NY), MG-132 and lactacystin (proteasome inhibitors), calpeptin (calpain inhibitor), cpm-VAD-CHO (caspase inhibitor), chloroquine (lysozyme inhibitor) were from Calbiochem (San Diego, CA). The neuroleptics clozapine, and halperidol, the pan-ErbB receptor antagonist PD158780 and MK-801 were from Tocris Biosciences (Ellisville, MO). The EGF domain and extracellular domain (ECD) of human NRG1β were from R&D Systems, (Minneapolis, MN). TC-2153 was synthesized as described(1). Antibodies are listed in **SI Table 4**. Primers are listed in **SI Table 5.**

hiPSCs.

Description of SZ patients. SZ1: All SZ fibroblasts were obtained from Coriell. Limited clinical information is available: Patient 1 (GM02038, male, 22 years of age, Caucasian) was diagnosed with SZ at six years of age and committed suicide at 22 years of age; Patient 2 (GM01792, male, 26 years of age, Jewish Caucasian) displayed episodes of agitation, delusions of persecution, and fear of assassination; his sister, Patient 3 (GM01835, female, 27 years of age, Jewish Caucasian), had a history of schizoaffective disorder and drug abuse; Patient 4 (GM02497, male, 23 years of age, Jewish Caucasian) was diagnosed with SZ at age 15 and showed symptoms including paralogical thinking, affective shielding, splitting of affect from content, and suspiciousness. Control fibroblasts were obtained from ATCC (Control 1, CRL-2522 (male, neonatal)) and Coriell (Control 2, GM03440 (male, 20 years of age); Control 3, GM03651 (female, 25 years of age); Control 4, GM04506 (female, 22 years of age); Control 5, AG09319 (female, 24 years of age); and Control 6, AG09429 (female, 25 years of age).

SZ2: Patients with childhood-onset-schizophrenia, unaffected family members and unrelated controls were recruited into a longitudinal study by Dr. Judith Rapoport (NIMH)(2-6), from which most have had fibroblast biopsies completed. The Rapoport laboratory at NIH generously provided SZ2 fibroblasts from nine cases and eight controls. The following controls were used: C1 (NSB553, male), C2 (NSB690, male), C3 (NSB2607, male), C4 (NSB3084, male), C5 (NSB3158, female), C6 (NSB3182, female), C7 (NSB3234, male), C8 (NSB3113, female). The following cases were used: P1 (NSB499, female), P2 (NSB581, male), P3 (NSB676, female), P4 (NSB1442, male), P5 (NSB2513, male), P6 (NSB2620, male), P7 (NSB2011, female), P8 (NSB2476, female), P9 (NSB2962, male).

To ensure accurate diagnosis, as transient psychotic symptoms are common across a spectrum of childhood disorders, Dr. Rapoport relies on medication-free in-patient observation(7). The following clinical information was collected: gender, age at biopsy, developmental history, age of symptom onset, IQ, number of hospitalizations as a measure of disease severity, positive and negative symptom scale, diagnostic screening by Comprehensive Assessment of Symptoms and History (CASH), attention tests, current antipsychotic treatment, clozapine responsiveness and substance abuse history. A developmental MRI time-course revealed reduced cortical thickness in SZ2 patients compared to controls; with increasing age, the SZ2 brain developmental trajectory normalized in parietal regions but remained divergent in frontal and temporal regions, a pattern of loss similar to adult-onset SZ(7) suggesting that SZ2 is continuous with the adult disorder. All samples have had IlluminaOmni 2.5 bead chip genotyping(8) and have also had PsychChip and exome sequencing completed at Icahn School of Medicine at Mount Sinai.

The SZ2 cohort represents a relatively homogeneous subset of SZ patients defined by onset, severity and prognosis. In adulthood, SZ2 patients resemble chronic poor outcome adult onset SZ (AOS); in fact, SZ2 is reliably diagnosed in children using unmodified DSM criteria(9). There are no clinical, neuroimaging, pharmacological or genetic data to suggest that childhood-onset-schizophrenia is a distinct disorder from adult-onset-schizophrenia (reviewed(10-12)).

HF culture and hiPSC derivation. SZ1 hiPSCs were derived as described previously(13). SZ2 human fibroblasts (HFs) were cultured on plates treated with 0.1% gelatin (in milli-Q water) for a minimum of 30 min and grown in HF media (DMEM (Life Technologies) + 20% FBS (Gemini)). SZ2 hiPSCs were derived as described previously(14); replicating but nearly confluent HFs were transfected once with Cytotune Sendai virus expressing OCT4, SOX2, KLF4 and cMYC (Life Technologies) and after 3-5 days of recovery, with TrypleE (Life Technologies) and re-plated onto a 10-cm dish containing 1 million mouse embryonic fibroblasts (mEFs). Cells were switched to HUES media (DMEM/F12 (Invitrogen), 20% KO-Serum Replacement (Invitrogen), 1x Glutamax (Invitrogen), 1x NEAA (Invitrogen), 1x 2-mercaptoethanol (Sigma) and 20 ng/ml FGF2 (Invitrogen)) and fed every 2-3 days. hiPSC colonies were manually picked and clonally plated onto 24-well mEF plates. hiPSC lines were either maintained on mEFs in HUES media or on Matrigel (BD) in TeSR media (Stemcell Technologies). At early passages, hiPSCs were split through manual passaging. At higher passages, hiPSC could be enzymatically passaged with Collagenase (1mg/ml in DMEM) (Life Technology). Cells were frozen in cold freezing media (HUES media, 10% DMSO). At approximately passage 10, karyotyping analysis was performed by Wicell Cytogenetics (Madison WI); only karyotypically normal lines were used for subsequent studies. All hiPSC lines were validated by: long-term expansion beyond 10 passages; FACS analysis for SSEA-4 and TRA-1-60 levels; and transcript analysis for *OCT4*,

NANOG, *c-MYC* and *LIN28*. For hiPSC validation using FACS, cells were dissociated using Accutase and MEF subtraction was performed as per (15) before a 30 min blocking step in 1% (w/v) bovine serum albumin (BSA) dissolved in PBS. Cells were labeled with TRA-1-60-488 (5ul per 1 x 10^6 cells, BioLegend #330613) and SSEA4-647 (5µl per 1 x 10^6 cells, BioLegend #33407) in 1% (w/v) BSA for 45 min at 4°C before being washed with 1 x PBS. Cells were resuspended in FACS buffer (1 x PBS (no Mg^{2+}/Ca^2) containing TO-PRO3® (ThermoFisher Scientific #T3605) and filtered using a 40 µm filter (BD Biosciences). Cytometry was performed using a LSR-II (BD Biosciences) and analysis was performed using Flowjo (v8.7.3 Treestar). hiPSC validation using transcript analysis, was carried out using a QuantStudio™ 7 Flex Real-Time PCR System using the Power SYBR green RNA-to-Ct RT-qPCR kit for primers (both ThermoFisher Scientific). 50 ng of RNA template was added to the PCR mix, containing primers detailed in **SI Table 5** (ThermoFisher Scientific). qPCR conditions were as follows, 48°C for 15 min, 95°C for 10 min followed by 40 cycles (95°C for 15 sec, 60°C for 60 sec).

hiPSC NPC culture. SZ1(13) and SZ2 (14) hiPSC forebrain NPCs were derived as described previously (16). Briefly, hiPSCs were incubated with Collagenase (1 mg/ml in DMEM) at 37°C for 1-2 hours until colonies lifted and could be transferred to a nonadherent plate (Corning). Embryoid Bodies (EBs) were grown in suspension in N2/B27 media (DMEM/F12-Glutamax (Invitrogen), 1x N2 (Invitrogen), 1X B27 (Invitrogen)); 7-day-old EBs were plated in N2/B27 media with 1 µg/ml Laminin (Invitrogen) onto poly-ornithine /Laminin-coated plates. Neural rosettes were harvested from 14-day-old EBs and re-plated in NPC media (DMEM/F12, 1x N2, 1x B27-RA (Invitrogen), 1 µg/ml Laminin and 20 ng/ml FGF2 on poly-ornithine/laminin-coated plates. SZ2 hiPSC NPCs (17) were generated in a similar method to SZ1 hiPSC NPCs (13, 18), except that they were i) differentiated with dual-SMAD inhibition (0.1µM LDN193189

(Stemgent) and 10μM SB431542 (Tocris)) (19) to improve yield and ii) harvested using STEMdiff™ Neural Rosette Selection Reagent (Stem Cell Technologies) for 60 minutes at 37°C (instead of manual picking). Forebrain NPCs were maintained at high density, grown on either Matrigel or Poly-Ornithine/Laminin-coated plates in NPC media (DMEM/F12, 1x N2, 1x B27-RA (Invitrogen), 1 μg/ml Laminin (Invitrogen) and 20 ng/ml FGF2 (Invitrogen) and split approximately 1:3-1:4 every week with Accutase (Millipore). NPCs could be expanded up to 10 passages. For SZ2 NPC validation NPCs were dissociated using Accutase, fixed for 10 min in 4% paraformaldehyde (PFA), permeabilized and blocked with 0.5% (v/v) Triton (Sigma)/1% (w/v) bovine serum albumin (BSA, Sigma) in PBS and labeled with NESTIN-647 (20μl per 1 x 10^6 NPCs, BD Biosciences #560393) and SOX2-488 (0.25 μg per 1 x 10^6 NPCs, BioLegend #656110) antibodies overnight at 4°C before being washed with 1 x PBS and resuspended in FACS buffer (1 x PBS (no Mg^{2+}/Ca^{2})) and filtered using a 40 μm filter (BD Biosciences). Cytometry was performed using a LSR-II or FACS Canto (BD Biosciences) and analysis was performed using Flowjo (v8.7.3, Treestar).

hiPSC directed forebrain neuronal differentiation. For neuronal differentiations, NPCs were dissociated with Accutase and plated in neural differentiation media (DMEM/F12, 1x N2, 1X B27-RA, 20 ng/ml BDNF (Peprotech), 20 ng/ml GDNF (Peprotech), 1 μM dibutyrl-cyclicAMP (Sigma), 200 nM ascorbic acid (Sigma) onto Poly-Ornithine/Laminin (SZ1) or Matrigel (SZ2)-coated plates(13). hiPSC forebrain neurons were differentiated for 6 weeks for all gene expression and biochemical experiments and 3 months for synaptic experiments. Notably, synapse maturation occurs most robustly in vitro when hiPSC neurons are cocultured with wildtype human astrocytes (Sciencell). 0.5% FBS was supplemented into neural differentiation

media for all astrocyte coculture experiments. Microarray and RNAseq comparisons of the control and SZ1 hiPSC NPCs(18, 20) and neurons(13) are publically available.

***Ngn2*-induced neuronal differentiation**. For *Ngn2*-induced neuronal differentiation, NPCs were dissociated with Accutase (Millipore) and plated at a density of 1.5 million cells per well of a 6-well plate in NPC media onto Matrigel-coated plates(21). 24 h after plating, the media was replaced, lentiviruses (prepared as described in(22)) were added (a TetO-mNgn2-T2A-PuroR (Addgene ID: 52047) together with a constitutive reverse tetracycline transactivator (rtTA) (Addgene ID:19780), both in third generation lentiviral vectors), and plates were spinfected for 1 h at 1000g. NPCs were incubated at 37°C for an additional 3-4 h before viruses were removed and media replaced with fresh NPC media. 24 h after spinfection, NPC media was supplemented with doxycycline (1 μg/ml; Sigma) to induce mNgn2-T2A-PuroR expression, then after 24 h of transgene induction, puromycin (1 μg/ml; Sigma) was added to the media for 24 h of selection. Finally, media was switched to neuron media and neurons were allowed to mature for 14 days; for the first 6 days only neuron media was supplemented with doxycycline; half-media changes were performed every other day.

Pharmacological or genetic manipulation of hiPSC neurons. For STEP inhibitor treatment, six-week-old hiPSC forebrain neurons were treated with 1 μM TC-2153 or DMSO for 1 h and then harvested immediately. For anti-psychotic treatment, 5-week-old hiPSC forebrain neurons were treated with 5 μM clozapine or 10 μM loxapine for 7 days and then harvested at 6 weeks of differentiation. For NRG1β EGF domain treatment, six-week-old hiPSC forebrain neurons were treated with 10 nM, Nrg1β (R&D systems, Minneapolis, MN) or PBS for 6 or 24 h. For shRNA knockdown of STEP, hiPSC forebrain neurons were transduced with either LV-shRNA-PTPN5 (sc-44128-V, Santa Cruz) or LV-GFP, 7 days prior to harvest at 6 weeks of differentiation.

Lentivirus was either purchased directly from Santa Cruz or prepared by adapting the packaging protocol(22) to polyethylenimine (PEI) (Polysciences, Inc, Warrington, PA)-transfection of HEK-293T cells. To measure ubiquitinated STEP, SZ1-FB hiPSC neurons were pretreated with MG-132 (10 μM) for 1 h, followed by the addition of NRG1β (10 nM, 6 h), without replacing MG-132. Neurons were lysed and ubiquitinated proteins isolated using Agarose-TUBE2 (Tandem Ubiquitin Binding Entity, LifeSensors, Malvern, PA) as described below for rat primary cortical neurons.

hiPSC multi-electrode array analysis (MEA). hiPSC NPCs were seeded at 120,000 cells/well onto a Matrigel-coated 24-well MEA plate (Axion). After 24 h, NPC medium was replaced with neuron medium. At either 14 or 21 days of differentiation, neurons were treated with TC-2153, 50 μM picrotoxin or appropriate vehicle controls. Recordings were taken at 21 and 28 days of differentiation; the MEA plate was loaded in the Axion Maestro MEA reader and the electrical activity of Ngn2-induced neurons was recorded and analyzed by the AxIS 2.0 software. For all experiments, in each condition, 6 replicates per NPC line were tested (*$P < 0.05$, ANOVA with Fisher's post-hoc, SZ1-FB: 4 patients). All MEA recordings were completed in neuron media, so as to better reflect *in vitro* culture conditions used in our other hiPSC experiments; it is possible that firing activity may differ in other media formulations.

Real-time quantitative PCR (qPCR).

Gene expression analysis was performed on passage-matched NPCs and neurons. Cells were lysed in RNA BEE (Tel-test, Inc). RNA was chloroform extracted, pelleted with isopropanol, washed with 70% ethanol and resuspended in water. RNA was treated with RQ1 RNase-free DNase (Promega) for 30 minutes at 37°C and then the reaction was inactivated by incubation with EGTA Stop buffer at 65°C for 10 minutes.

Total RNA from WT and $Nrg1^{+/-}$ mouse frontal cortices was extracted using RNeasy lipid tissue kit (Qiagen, Valencia, CA) following the manufacturer's instructions. RNA quantification was done by a nanodrop spectrophotometer (Thermo Scientific, Wilmington, DE) and 1 μg of total RNA was used in reverse transcription reactions to obtain complimentary DNA (cDNA) using a Quanti Tech reverse transcription kit (Qiagen). Real-time quantitative PCR was performed in 96-well plates using a StepOnePlus Real-Time PCR Systems (v2.3, Applied Biosystems) kit and Syber Green PCR master mix (Applied Biosystems, Carlsbad, CA). Levels of $STEP_{61}$ mRNAs were normalized to glyceraldehyde-3-phosphate dehydrogenase (GAPDH) mRNA. All primers were listed in **SI Table 5**.

Treatment of rat cortical neurons. Neuronal cultures were maintained in Neurobasal with B27 supplement (Invitrogen, San Diego, CA) for 14 days until treatment. Cultures were preincubated with various inhibitors (PD158780, 10 μM; calpeptin, 10 μM; cpo-VAD-CHO, 10 μM; chloroquine, 500 μM; lactacystin, 5 μM) for 30 min, followed by NRG1β EGF domain treatment (10 nM, 30 min).

Measurement of ubiquitinated STEP. Rat cortical neurons were pretreated with MG-132 (10 μM) for 1 h, followed by NRG1β treatment (10 nM, 30 min). Neurons were lysed in lysis buffer (50mM Tris-HCl, pH 7.5, 150 mM NaCl, 1mM EDTA, 1% NP-40, 10 mM N-ethylmaleimide, 10 μM MG-132, 10% glycerol with complete protease inhibitor and phosphatase inhibitor tablets (Roche). Ubiquitinated proteins were isolated using Agarose-TUBE2 (Tandem Ubiquitin Binding Entity, LifeSensors, Malvern, PA) according to the manufacturer's protocol and as described(23). For some experiments, STEP species were immunoprecipitated using a monoclonal anti-STEP antibody (clone 23E5)(24, 25) and protein A/G-agarose beads (Santa

Cruz Biotechnology, Santa Cruz, CA). Ubiquitinated STEP species were visualized by probing with anti-ubiquitin antibody.

Surface biotinylation. After treatment, neurons were labeled with EZ-Link Sulfo-NHS-SS-Biotin (Pierce, Rockford, IL) as described(23, 26). Neurons were lysed in lysis buffer (50mM Tris-HCl, pH 7.5, 150 mM NaCl, 1 mM EDTA, 1% NP-40, with complete protease inhibitor and phosphatase inhibitor tablets) and lysates were incubated with NeutrAvidin agarose (Pierce) to isolate biotinylated proteins.

Sample preparation and western blot analysis. Cells were isolated, suspended in 1× RIPA lyses buffer (Sigma) supplemented with 1% complete protease inhibitor tablet per 50 mL and 1 phosSTOP phosphatase inhibitor tablet per 10 mL (Roche), triturated and centrifuged at 10,000 × g for 10 min at 4°C. Frontal cortices were collected after drug administration and processed by differential centrifugation to get crude synaptosomal membrane fractions (P2) as described (23). Thirty μg of total protein was separated on 8% SDS-polyacrylamide gel, transferred to a nitrocellulose membrane and probed with primary and horseradish-peroxidase-conjugated second antibodies (Supplementary Table 4). Blots were developed with a Chemiluminescent Substrate kit (Pierce) and visualized by a G:BOX with the GeneSnap software (Syngene, Cambridge, UK). All densitometric bands were quantified with the Genetools program (Syngene). For Western blotting, phosphorylated protein levels were normalized to total protein levels, then to β-actin as loading control, with one exception: when pGluN2B was evaluated in synaptosomal fractions (P2), pGluN2B levels were normalized to β-actin directly.

Mouse behavioral and cognitive assays. Four cohorts of male $Nrg1^{+/-}$ and WT littermates (6-9 months old, n = 9-16 each group) and two cohorts of male WT mice (C57BL6/J, 4-6 months old, n = 8-10 each group) were used for all the tests. Mice were administered vehicle (Veh), TC-2153

(TC, 10 mg/kg, i.p.) or clozapine (Clz, 1 mg/kg, i.p.). For locomotion, mice were pretreated with vehicle, TC-2153 or clozapine, followed by treatment with phencyclidine (PCP, 7.5 mg/kg, i.p.) or MK-801 (0.15 mg/kg, i.p.) acutely. Cohort 1 was tested in open-field and PCP-induced locomotor activity as described(1, 27). Cohort 2 was tested in Y-maze and novel object recognition (NOR) after PCP treatment as described(1, 23, 27). Cohort 3 was tested in social dominance and 3-chamber social tasks after PCP treatment as described (28). Cohort 4 was tested for PPI after PCP treatment. Cohort 5 was tested in MK-801 induced locomotor activity. Cohort 6 was tested in Y-maze and NOR after MK-801 treatment.

Locomotor activity. Mice were placed in an activity chamber (MED Associates, St. Albans, VT) for 30 min to obtain base line, followed by PCP (7.5 mg/kg, i.p.) injections, and monitored for an additional 1 h. Horizontal activity and stereotypies (such as sniffing, rearing and grooming) were measured using the Activity Monitor version 5 software (MED Associates) as described(23, 29).

Y-maze. The Y-maze apparatus consisted of three equal arms (42 × 4.8 × 20 cm). Mice were randomly placed at the end of one arm and allowed to freely explore the maze for 5 min. The total number of arm entries and alternation behavior were recorded and calculated using ANY-maze software as described(1, 27).

Novel object recognition (NOR). NOR was performed as described(1, 27). Mice were habituated to an open-field box for 10 min. Twenty-four h later (2^{nd} day), mice were trained with two identical objects and allowed to explore both for a total of 30 sec. Twenty-four h after training (3^{rd} day), mice were tested with a previous object (familiar) and a novel one. The location of objects was counter balanced to minimize bias. Time spent with the novel or familiar object was analyzed using ANY-maze.

Social dominance test. Age-matched non-littermate WT mice were used as controls for other groups ($Nrg1^{+/-}$, $STEP^{-/-}$ and DM mice) as described(28). Mice were placed in a head-to-head position at the opposite ends of a clear plastic tube (30.5 cm long × 3.8 cm inner diameter). Tests ended when one mouse retreated or the test time was over (2 min). The remaining mouse was judged as the winner. Each mouse performed 4 matches and % win was calculated.

Social interaction test. Social interaction was evaluated in a three-chamber apparatus as described(28). The apparatus consisted of a non-transparent plexiglass box (64 cm long × 43 cm wide × 38 cm tall), divided into three compartments (20 cm long × 43 cm wide) with small entryways to each chamber. The task consisted of three 10 min stages: (1) habituation, (2) social preference, and (3) social novelty. During habituation, the test mouse was placed in the center chamber and allowed to explore 2 empty cups located in the left and right chambers. During social preference, an age-matched non-littermate WT mouse was placed under the cup in the left or right chamber. The test mouse was allowed to freely explore the entire apparatus. A socialization index (interaction with the mouse within 1 inch margin around the cup, entries and duration of interaction) was recorded and calculated using ANY-maze. During social novelty, another strange mouse (age-matched, non-littermate WT) was kept under the empty cup, which was previously empty during social preference. The test mouse was allowed to make choices between the familiar and the novel mouse. Close proximity within a 1-inch margin around the cup with either mouse was considered as interaction.

PPI test. WT and $Nrg1^{+/-}$ were administered with vehicle (Veh, 2% DMSO in saline) or TC-2153 (TC, 10 mg/kg in saline, i.p.) 3 h prior to test. Same group of mice were tested twice with 1-week break (drug wash out), counterbalanced by genotype and treatment. Data were organized using Microsoft Excel and analyzed using SPSS (IBM). Repeated-measure (RM)-ANOVA was

used to analyze PPI data, and the threshold for significance was set at alpha = 0.05. $Nrg1^{+/-}$ N=10, and WT N=10.

SI REFERENCES

1. Xu J, Chatterjee M, Baguley TD, Brouillette J, Kurup P, Ghosh D, et al. (2014): Inhibitor of the tyrosine phosphatase STEP reverses cognitive deficits in a mouse model of alzheimer's disease. *PLoS Biol*. 12:e1001923.

2. Sporn A, Addington A, Reiss AL, Dean M, Gogtay N, Potocnik U, et al. (2004): 22q11 deletion syndrome in childhood onset schizophrenia: an update. *Mol Psychiatry*. 9:225-226.

3. Shaw P, Sporn A, Gogtay N, Overman GP, Greenstein D, Gochman P, et al. (2006): Childhood-onset schizophrenia: A double-blind, randomized clozapine-olanzapine comparison. *Arch Gen Psychiatry*. 63:721-730.

4. McCarthy SE, Makarov V, Kirov G, Addington AM, McClellan J, Yoon S, et al. (2009): Microduplications of 16p11.2 are associated with schizophrenia. *Nat Genet*. 41:1223-1227.

5. Gogtay N, Giedd JN, Lusk L, Hayashi KM, Greenstein D, Vaituzis AC, et al. (2004): Dynamic mapping of human cortical development during childhood through early adulthood. *Proc Natl Acad Sci U S A*. 101:8174-8179.

6. Eckstrand K, Addington AM, Stromberg T, Merriman B, Miller R, Gochman P, et al. (2008): Sex chromosome anomalies in childhood onset schizophrenia: an update. *Mol Psychiatry*. 13:910-911.

7. Greenstein D, Lerch J, Shaw P, Clasen L, Giedd J, Gochman P, et al. (2006): Childhood onset schizophrenia: cortical brain abnormalities as young adults. *J Child Psychol Psychiatry*. 47:1003-1012.

8. Ahn K, Gotay N, Andersen TM, Anvari AA, Gochman P, Lee Y, et al. (2014): High rate of disease-related copy number variations in childhood onset schizophrenia. *Mol Psychiatry*. 19:568-572.

9. McKenna K, Gordon CT, Rapoport JL (1994): Childhood-onset schizophrenia: timely neurobiological research. *J Am Acad Child Adolesc Psychiatry*. 33:771-781.

10. Gordon CT, Frazier JA, McKenna K, Giedd J, Zametkin A, Zahn T, et al. (1994): Childhood-onset schizophrenia: an NIMH study in progress. *Schizophr Bull*. 20:697-712.

11. Rapoport JL, Giedd JN, Gogtay N (2012): Neurodevelopmental model of schizophrenia: update 2012. *Mol Psychiatry*. 17:1228-1238.

12. Rapoport JL, Addington AM, Frangou S, Psych MR (2005): The neurodevelopmental model of schizophrenia: update 2005. *Mol Psychiatry*. 10:434-449.

13. Brennand KJ, Simone A, Jou J, Gelboin-Burkhart C, Tran N, Sangar S, et al. (2011): Modelling schizophrenia using human induced pluripotent stem cells. *Nature*. 473:221-225.

14. Lee IS, Carvalho CMB, Douvaras P, Ho SM, Hartley BJ, Zuccherato LW, et al. (2015): Characterization of molecular and cellular phenotypes associated with a heterozygous CNTNAP2 deletion using patient-derived hiPSC neural cells. *NPJ Schizophrenia*. 1:15019.

15. Kriks S, Shim JW, Piao J, Ganat YM, Wakeman DR, Xie Z, et al. (2011): Dopamine neurons derived from human ES cells efficiently engraft in animal models of Parkinson's disease. *Nature*. 480:547-551.

16. Topol A, Tran NN, Brennand KJ (2015): A guide to generating and using hiPSC derived NPCs for the study of neurological diseases. *Journal of visualized experiments : JoVE*.e52495.

17. Topol A, Zhu S, Hartley BJ, English J, Hauberg ME, Tran N, et al. (2016): Dysregulation of miRNA-9 in a Subset of Schizophrenia Patient-Derived Neural Progenitor Cells. *Cell reports*. 15:1024-1036.

18. Brennand K, Savas JN, Kim Y, Tran N, Simone A, Hashimoto-Torii K, et al. (2015): Phenotypic differences in hiPSC NPCs derived from patients with schizophrenia. *Mol Psychiatry*. 20:361-368.

19. Chambers SM, Fasano CA, Papapetrou EP, Tomishima M, Sadelain M, Studer L (2009): Highly efficient neural conversion of human ES and iPS cells by dual inhibition of SMAD signaling. *Nat Biotechnol*. 27:275-280.

20. Topol A, Zhu S, Tran N, Simone A, Fang G, Brennand KJ (2015): Altered WNT Signaling in Human Induced Pluripotent Stem Cell Neural Progenitor Cells Derived from Four Schizophrenia Patients. *Biol Psychiatry*. 78:e29-34.

21. Ho SM, Hartley BJ, Tcw J, Beaumont M, Stafford K, Slesinger PA, et al. (2016): Rapid Ngn2-induction of excitatory neurons from hiPSC-derived neural progenitor cells. *Methods*. 101:113-124.

22. Tiscornia G, Singer O, Verma IM (2006): Production and purification of lentiviral vectors. *Nat Protoc*. 1:241-245.

23. Carty NC, Xu J, Kurup P, Brouillette J, Goebel-Goody SM, Austin DR, et al. (2012): The tyrosine phosphatase STEP: implications in schizophrenia and the molecular mechanism underlying antipsychotic medications. *Translational psychiatry*. 2:e137.

24. Lombroso PJ, Naegele JR, Sharma E, Lerner M (1993): A protein tyrosine phosphatase expressed within dopaminoceptive neurons of the basal ganglia and related structures. *JNeurosci*. 13:3064-3074.

25. Paul S, Nairn AC, Wang P, Lombroso PJ (2003): NMDA-mediated activation of the tyrosine phosphatase STEP regulates the duration of ERK signaling. *Nat Neurosci*. 6:34-42.

26. Kurup P, Zhang Y, Xu J, Venkitaramani DV, Haroutunian V, Greengard P, et al. (2010): Abeta-mediated NMDA receptor endocytosis in Alzheimer's disease involves ubiquitination of the tyrosine phosphatase STEP61. *J Neurosci*. 30:5948-5957.

27. Zhang Y, Kurup P, Xu J, Carty N, Fernandez SM, Nygaard HB, et al. (2010): Genetic reduction of striatal-enriched tyrosine phosphatase (STEP) reverses cognitive and cellular deficits in an Alzheimer's disease mouse model. *Proc Natl Acad Sci U S A*. 107:19014-19019.

28. Goebel-Goody SM, Wilson-Wallis ED, Royston S, Tagliatela SM, Naegele JR, Lombroso PJ (2012): Genetic manipulation of STEP reverses behavioral abnormalities in a fragile X syndrome mouse model. *Genes, brain, and behavior*. 11:586-600.

29. Xu J, Kurup P, Baguley TD, Foscue E, Ellman JA, Nairn AC, et al. (2015): Inhibition of the tyrosine phosphatase STEP restores BDNF expression and reverses motor and cognitive deficits in phencyclidine-treated mice. *Cellular and molecular life sciences : CMLS*.

Supplemental Figure and Tables

SI Figures:

SI Tables:

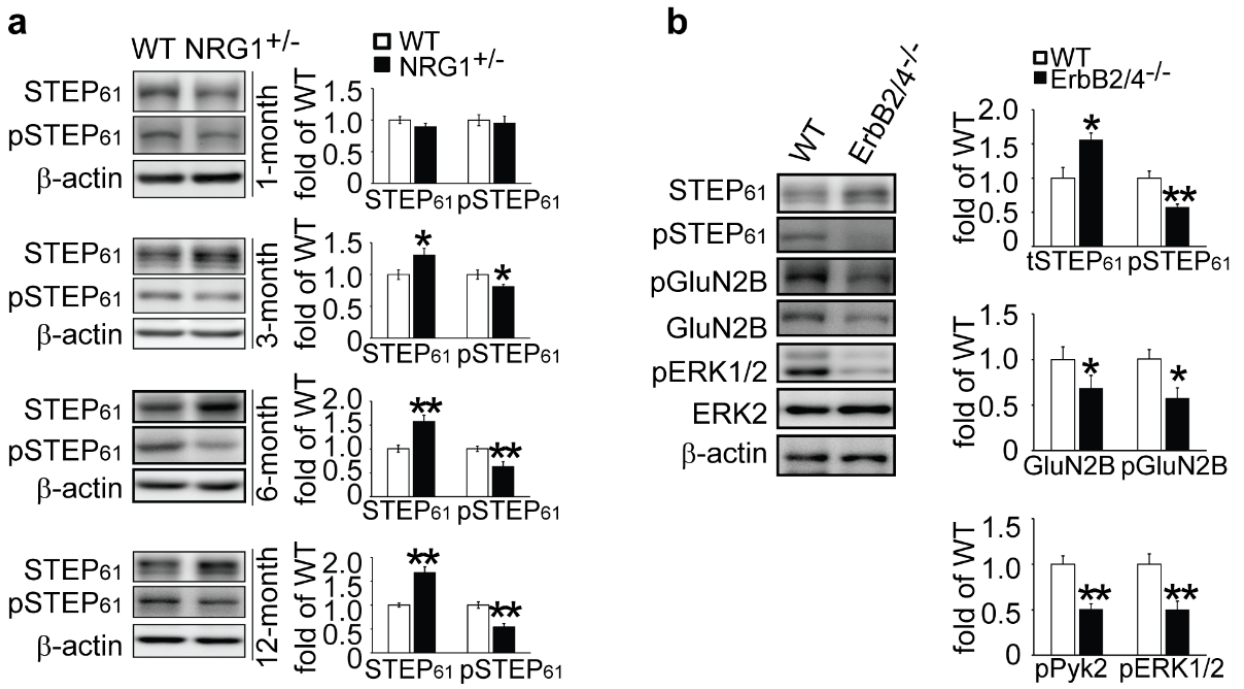

SI Figure 1. $STEP_{61}$ is elevated in $Nrg1^{+/-}$ and $ErbB2/4^{-/-}$ mice. (**a**) Male WT and $Nrg1^{+/-}$ littermates were collected at 1, 3, 6 and 12 months. P2 fractions from frontal cortices were processed by WB for $STEP_{61}$ and $pSTEP_{61}$ levels. (**b**) P2 fractions from $ErbB2/4^{-/-}$ mice (9 months old) were processed by WB using antibodies against total $STEP_{61}$, phosphorylated $STEP_{61}$ ($pSTEP_{61}$, inactive) and tyrosine phosphoryledGluN2B and ERK1/2. All antibodies were listed in **SI Table 4**. All data were expressed as mean ± SEM and statistical significance was determined using Student *t*-test (**P* < 0.05, ***P* < 0.01, n = 6 for **a**; n = 3 for **b**).

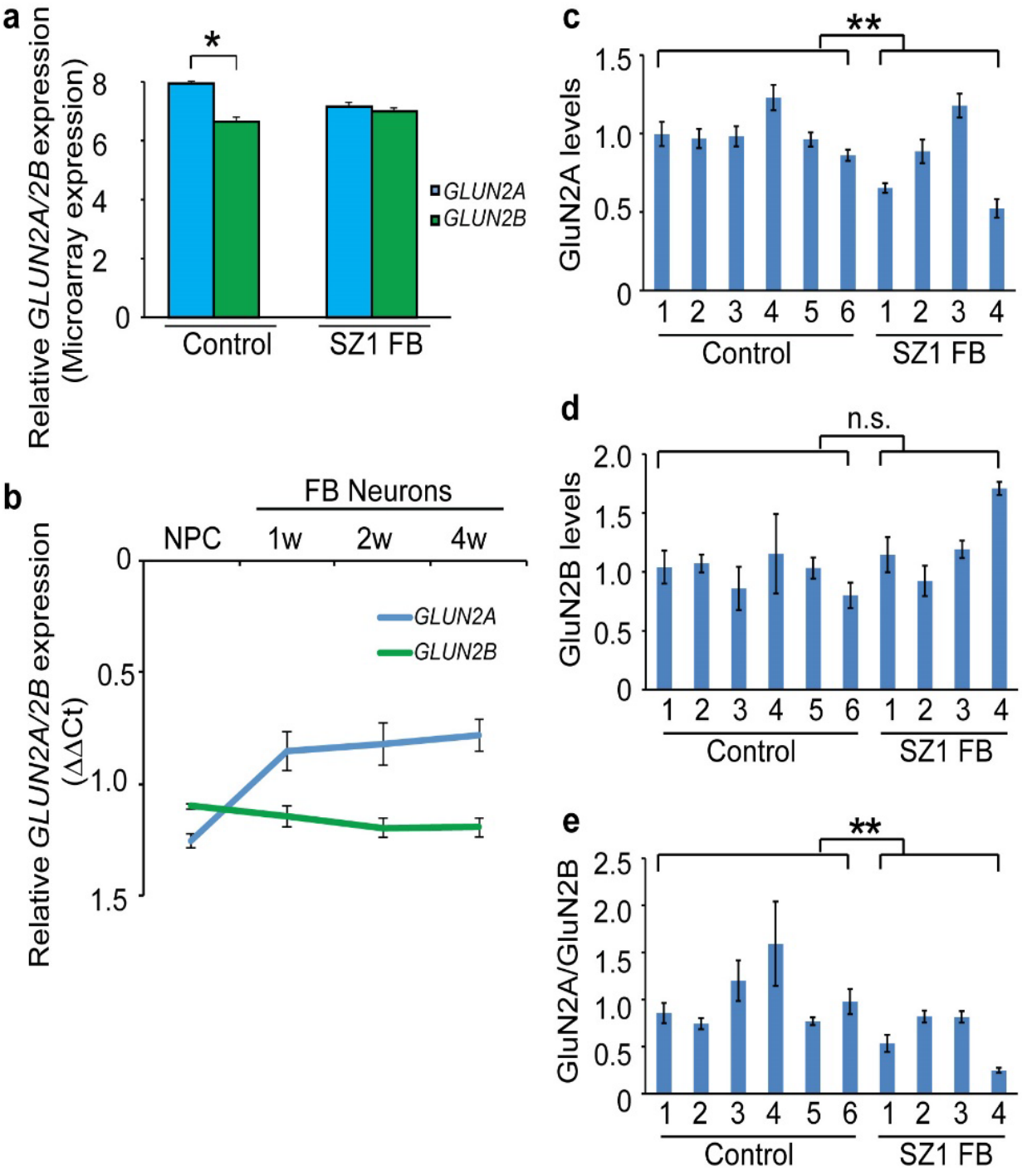

SI Figure 2. GluN2A/GluN2B subunit ratio is decreased in SZ1 forebrain neurons. (**a**) Microarray expression data of normalized *GluN2A/GluN2B* expression of control and SZ1 FB neurons. (**b**) qPCR of *GluN2A/GluN2B* expression ratio during neuronal differentiation of two

independent control NPC lines into 1-, 2-, and 4-week-old forebrain (FB) neurons. (**c-e**) SZ1 control and forebrain (FB) neuronal lysates were probed for GluN2A (**c**) and GluN2B (**d**) levels. GluN2A/GluN2B ratio (**e**) was also analyzed. Data were expressed as mean ± SEM from 3-6 replicates and statistical significance was determined by nested analyses using JMP (**$P < 0.01$, 6 controls and 4 patients).

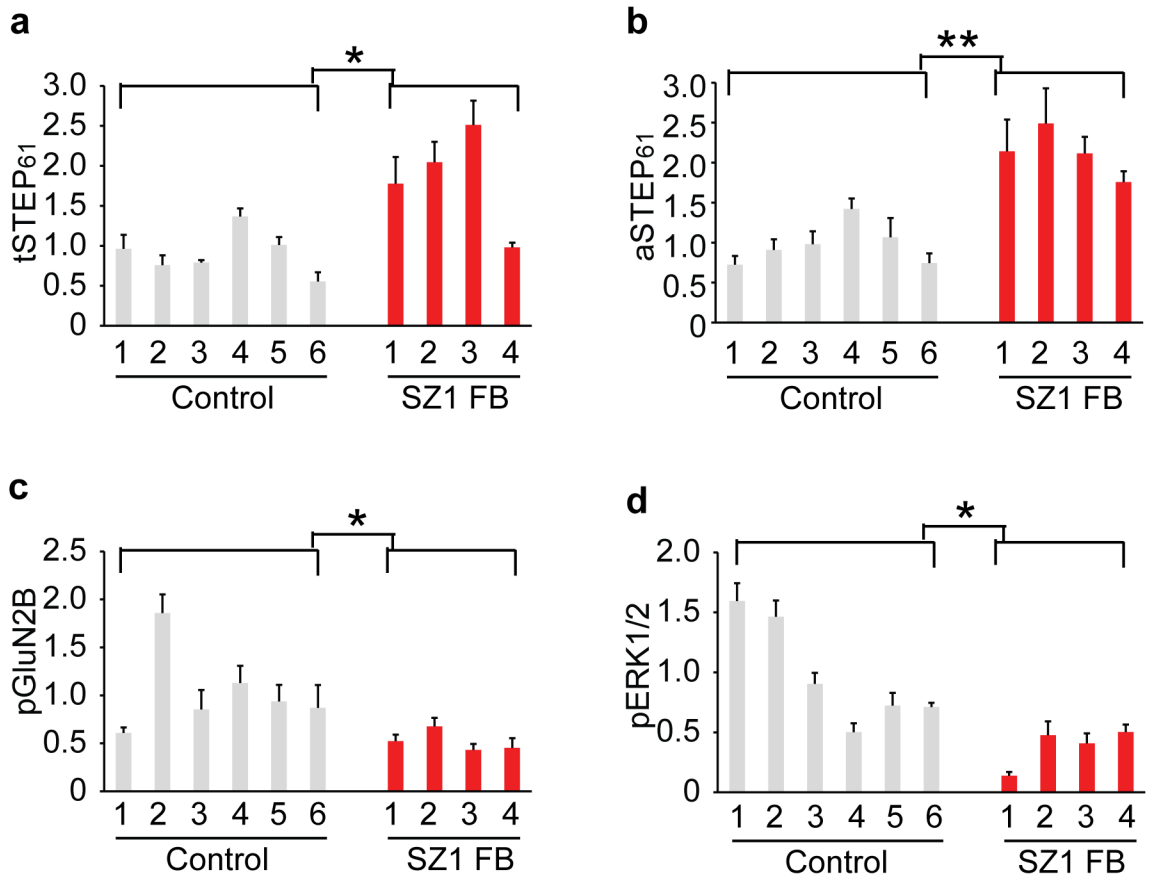

SI Figure 3. $STEP_{61}$ levels and phosphorylation of its substrates in SZ1-FB hiPSC neurons by individual. (**a-d**): Increased basal levels of total (**a**) and active (**b**) $STEP_{61}$ levels in SZ1-FB neurons correlated with decreased levels of the $STEP_{61}$ substrates pGluN2B (**c**) and pERK1/2 (**d**). All data were expressed as mean ± SEM and statistical significance was determined by JMP nested analysis using standard least squares analysis, followed by Student *t*-test (**P* < 0.05, ***P* < 0.01, n = 3-6 biological replicates for each case).

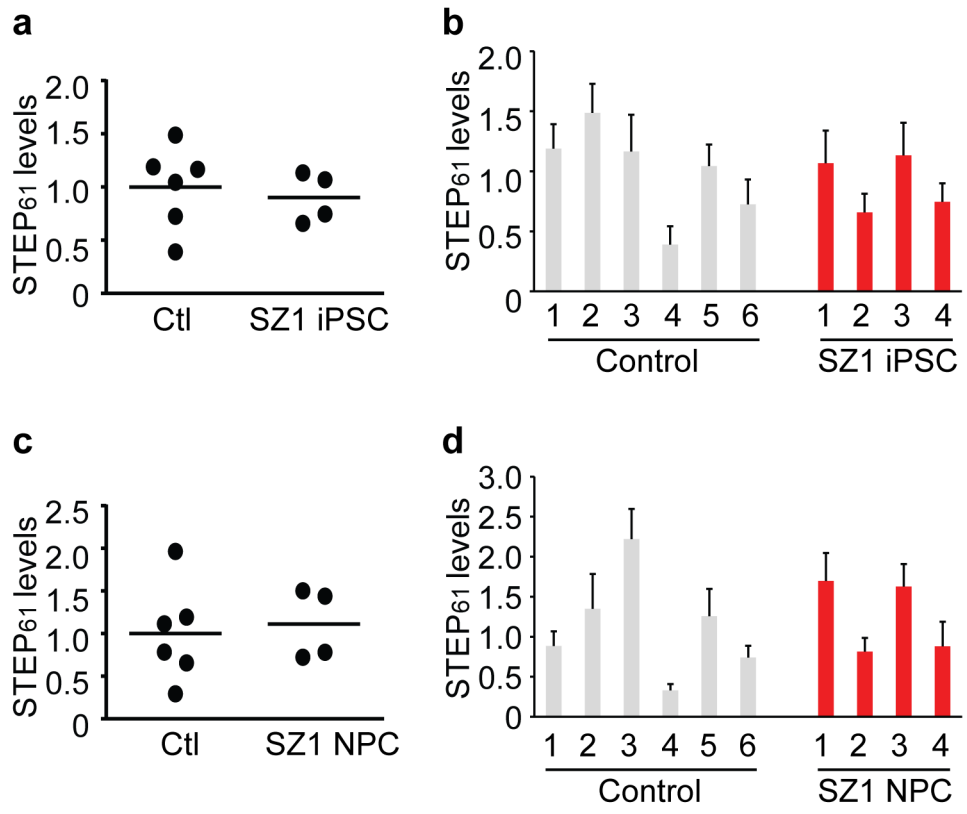

SI Figure 4. $STEP_{61}$ levels do not change in SZ1 hiPSCs or NPCs. Western blot analysis of $STEP_{61}$ protein levels, relative to β-ACTIN. (**a-d**) No differences in basal levels of total $STEP_{61}$ levels in SZ1 hiPSCs (by group average (**a**) or by individual (**b**)). No differences in basal levels of total $STEP_{61}$ levels in SZ1 hiPSC forebrain NPCs (by group average (**c**) or by individual (**d**)). All data were expressed as mean ± SEM and statistical significance was determined by JMP nested analysis using standard least squares analysis, followed by Student *t*-test (n = 3-6 biological replicates for each case).

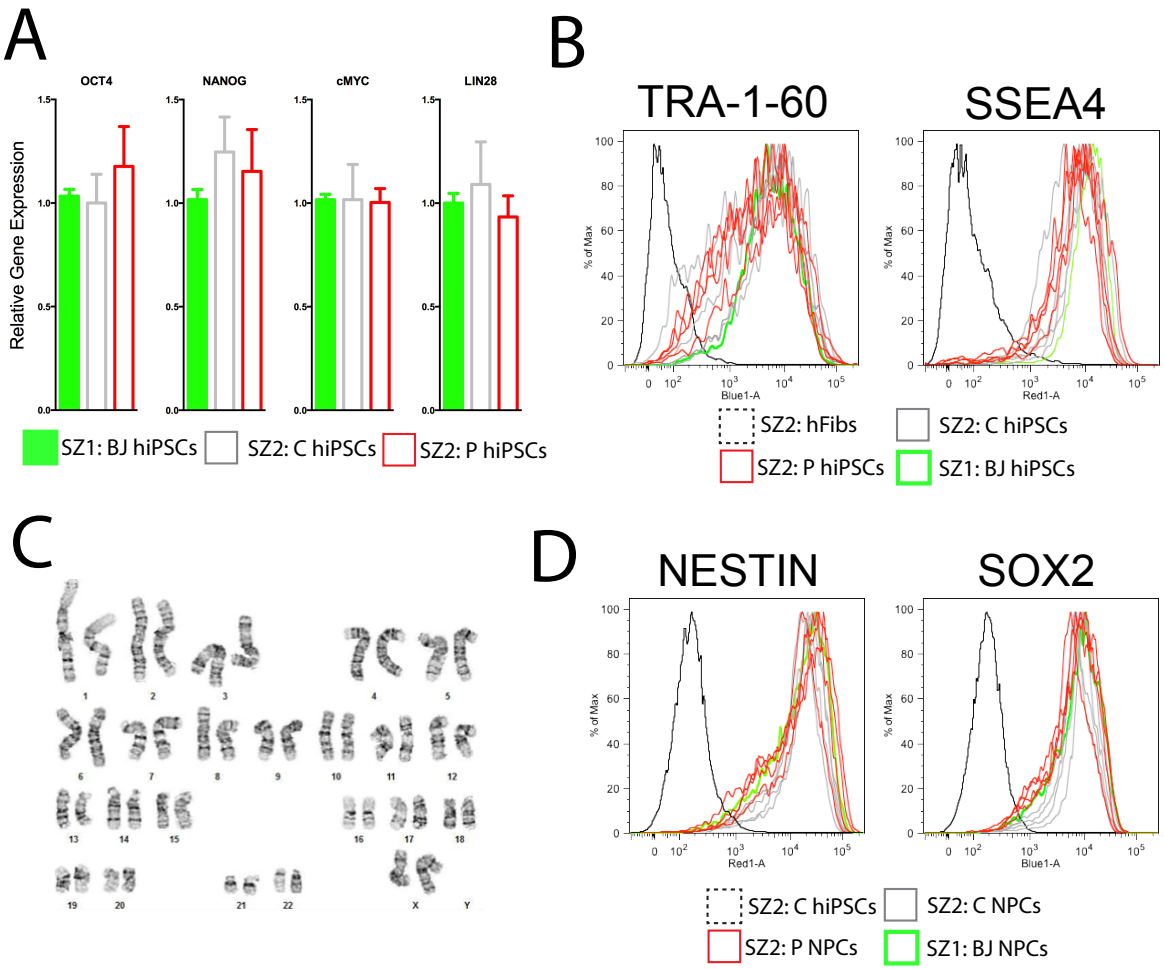

SI Figure 5. Validation of SZ2 hiPSCs and NPCs, **A.** Relative gene expression (qPCR) of human pluripotency markers C-MYC, OCT4, NANOG and LIN-28, normalized to GAPDH and β-ACTIN from hiPSCs derived from both control (C, grey unfilled bar) and childhood-onset-SZ (COS) patient (P, unfilled bar) SZ cohort 2 (SZ2) fibroblasts and a previously validated BJ (ATCC CRL-2522) hiPSC line (green filled bar) (SZ1). **B.** TRA-1-60-488 (left panel) and SSEA4-647 (right panel) FACS histograms. Black dotted line (SZ2:1 control fibroblast cell line), grey lines (SZ2: 4 individual control hiPSC lines) red lines (SZ2: 4 individual COS hiPSC lines) and green thick line (SZ1: previously validated BJ (ATCC CRL-2522) hiPSC line. **C**. A representative karyotype image from a SZ2 P fibroblast derived hiPSC line showing no chromosomal abnormalities. **D:** NESTIN-647 (left panel) and SOX2-488 (right panel) FACS

histograms. Black dotted line (SZ2:1 control hiPSC cell line), grey lines (SZ2: 4 individual control NPC lines) red lines (SZ2: 4 individual COS NPC lines) and green thick line (SZ1: previously validated BJ-2A (Brennand et al., 2011) hiPSC line.

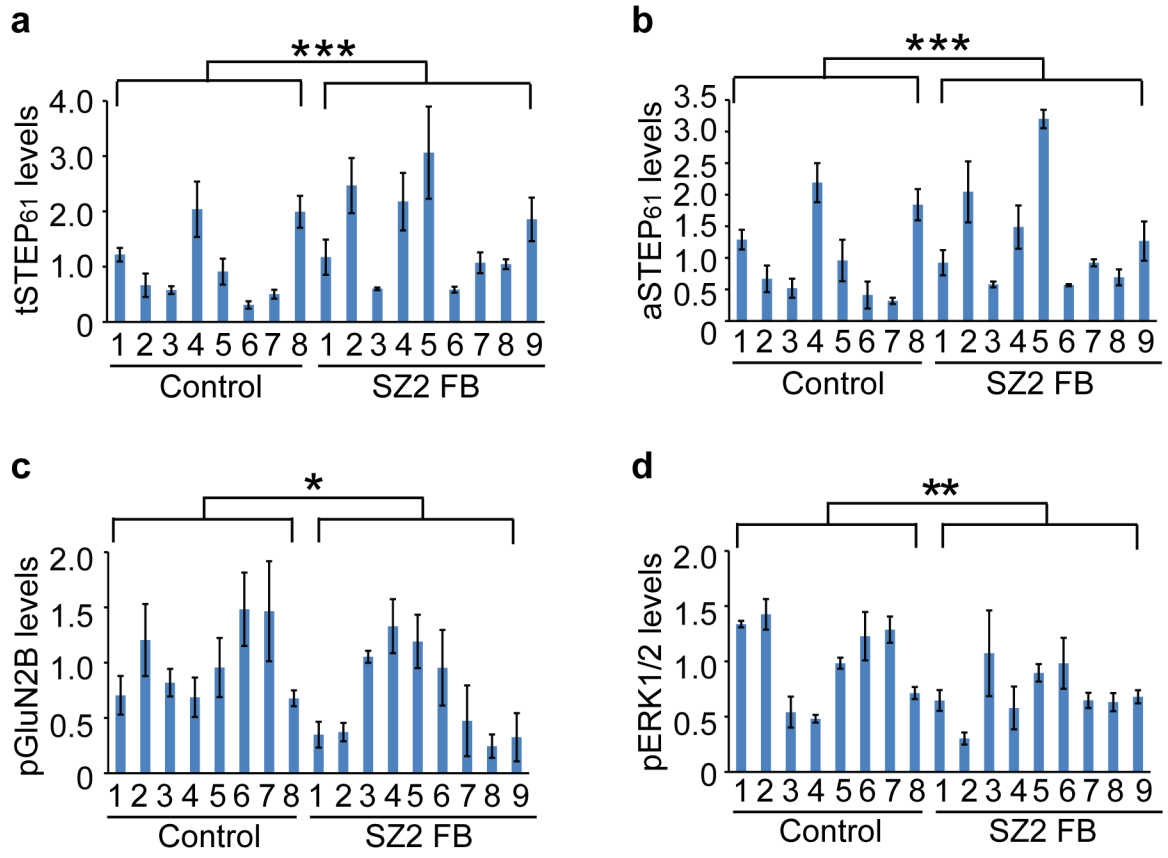

SI Figure 6. $STEP_{61}$ levels and phosphorylation of its substrates in SZ2-FB hiPSC neurons by individual. (**a-d**): Increased basal levels of total (**a**) and active (**b**) $STEP_{61}$ levels in SZ2-FB hiPSC neurons correlates with decreased levels of the $STEP_{61}$ substrates pGluN2B (**c**) and pERK1/2 (**d**). All data were expressed as mean ± SEM and statistical significance was determined by JMP nested analysis using standard least squares analysis, followed by Student *t*-test (*$P < 0.05$, **$P < 0.01$, ***$P < 0.001$, n = 3-6 biological replicates for each case).

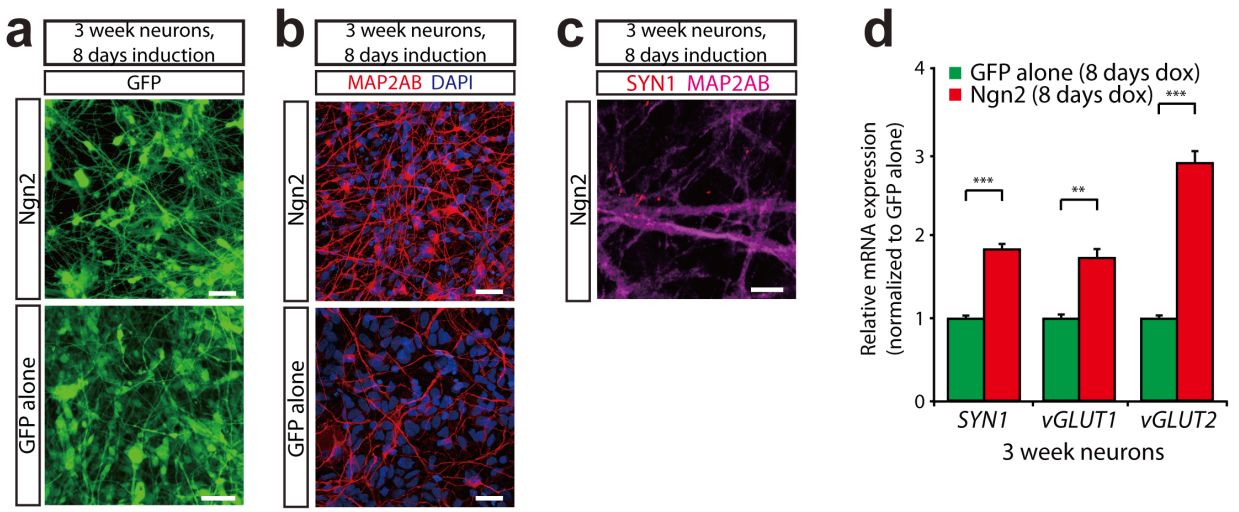

SI Figure 7. Validation of transient *Ngn2*-induction of SZ2-GLU neurons. Three-week-old *Ngn2*-neurons were used for all experiments; *Ngn2*-expression was transiently induced from days 1-8. (**a**) GFP images of live Ngn2- and GFP-transduced NPCs, showing that *Ngn2*-inductions lead to faster acquisition of neuronal morphology. Scale bar 50 μm. (**b**) Representative images of Ngn2-induced neurons and GFP-NPCs at three weeks of age, stained with neuronal dendrite marker MAP2AB (red) and DAPI-stained nuclei (blue). Scale bar 30 μm. (**c**) Representative image of *Ngn2*-neurons at three weeks of age, stained with presynaptic marker SYN1 (red) and MAP2AB (magenta). Scale bar 4 μm. (**d**) Real-time qPCR analysis of SYN1, vGLUT1 and vGLUT2 mRNA expression between three-week-old GFP-NPCs and three-week-old Ngn2-induced neurons, each with 7 days of doxycycline exposure. Error bars are SEM. **P < 0.01, ***P < 0.001.

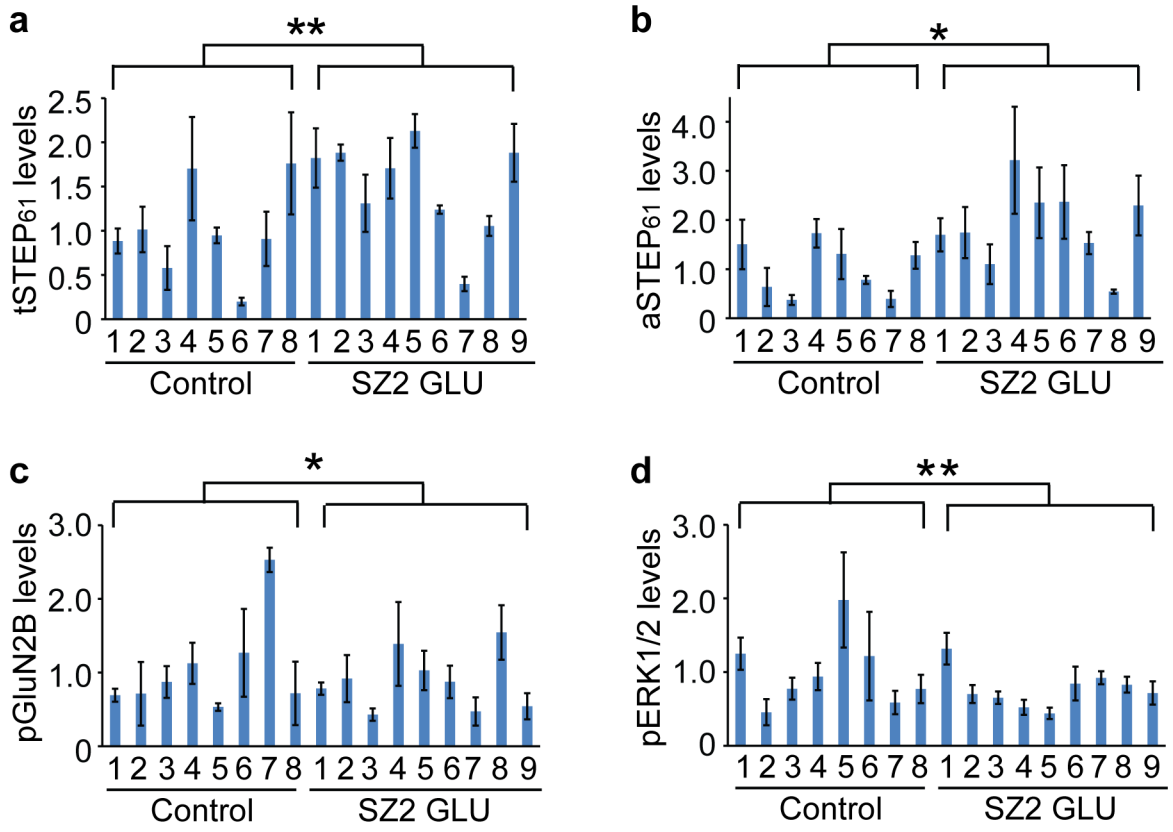

SI Figure 8. $STEP_{61}$ levels and phosphorylation of its substrates in SZ2-GLU hiPSC neurons by individual. (**a-d**): Increased basal levels of total (**a**) and active (**b**) $STEP_{61}$ levels in SZ2-GLU hiPSC neurons correlates to decreased levels of the $STEP_{61}$ substrates pGluN2B (**c**) and pERK1/2 (**d**). All data were expressed as mean ± SEM and statistical significance was determined by JMP nested analysis using standard least squares analysis, followed by Student *t*-test (*$P < 0.05$, **$P < 0.01$, n = 3-6 biological replicates for each case).

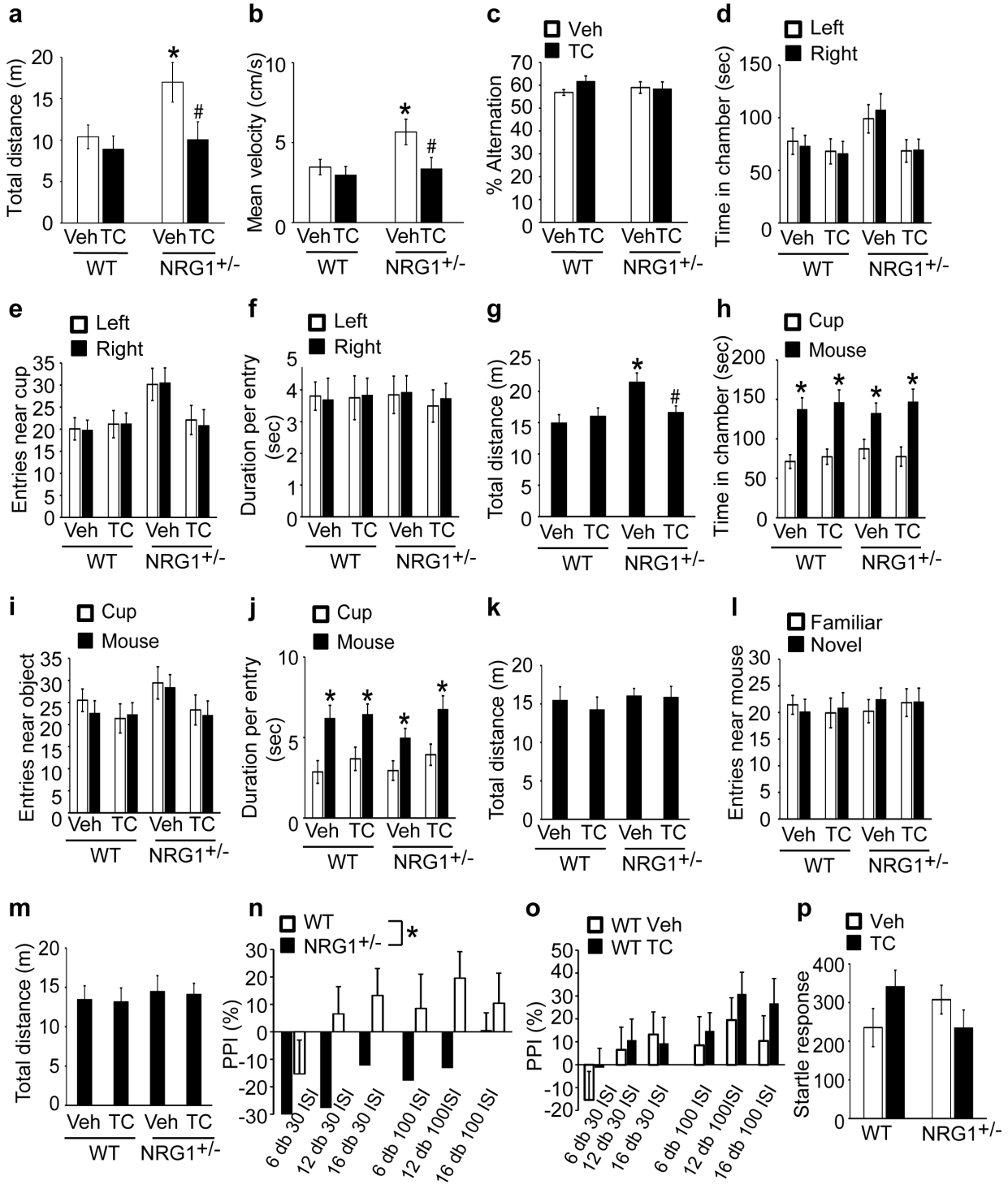

SI Figure 9. STEP inhibitor reverses hyperactivity in Nrg1$^{+/-}$ mice. Male WT and Nrg1$^{+/-}$ littermates (6-9 months old, 9-16 mice each group) were used for all tests. TC-2153 (TC, 10 mg/kg, i.p.) or vehicle (Veh) were administered 3 h prior to behavioral tests. (**a, b**) TC-2153

reverses basal hyperactivity in Nrg1$^{+/-}$ mice. Mice were allowed to freely explore in an open-field for 5 min. Total distance (**a**) and mean velocity (**b**) were calculated using ANY-maze. (**c**) Nrg1$^{+/-}$ mice did not differ from WT mice in Y-maze alternation task. Mice were tested in Y-maze for 5 min. Alternation to any arm was calculated using ANY-maze. (**d-g**) TC-2153 reverses hyperactivity in Nrg1$^{+/-}$ mice during habituation of 3-chamber social interaction. Mice were placed in the center chamber and allowed to explore all three chambers for 10 min. Two empty cups were kept in the left and right chambers. Time spent in each chamber and in close proximity (within 1 inch) to either cups, and total distance traveled during the test was recorded using ANY-maze. (**h-k**) Nrg1$^{+/-}$ mice did not show deficits in social novelty. After habituation, mice were placed in the center chamber, with one empty cup and one strange mouse in the left and right chambers. Mice were allowed to explore all three chambers for 10 min. Close proximity within 1 inch around the cup that has the strange mouse under it was considered as social interaction. Social behaviors were recorded using ANY-maze. (**l, m**) Nrg1$^{+/-}$ mice did not differ from WT mice in total entries and total distance traveled during social novelty phase. (**n**) Nrg1$^{+/-}$ mice displayed deficits in PPI compared with WT. (**o**) TC-2153 did not alter PPI in WT mice. (**p**)WT and Nrg1$^{+/-}$ mice had similar startle response upon TC-2153 or vehicle treatment. All data were expressed as mean ± SEM and statistical significance was determined using two-way ANOVA with Bonferroni *post hoc* test for (**a, b**), one-way ANOVA with Bonferroni *post hoc* test for (**g, k, m**), Repeated-measure (RM)-ANOVA for (**n, o**), one-way ANOVA for (**p**) or Student *t*-test comparing two objects (**d-f, h-j, l**) (*$P < 0.05$; $^{\#}P < 0.05$, compared with Nrg1$^{+/-}$ group, n = 9-16 per group).

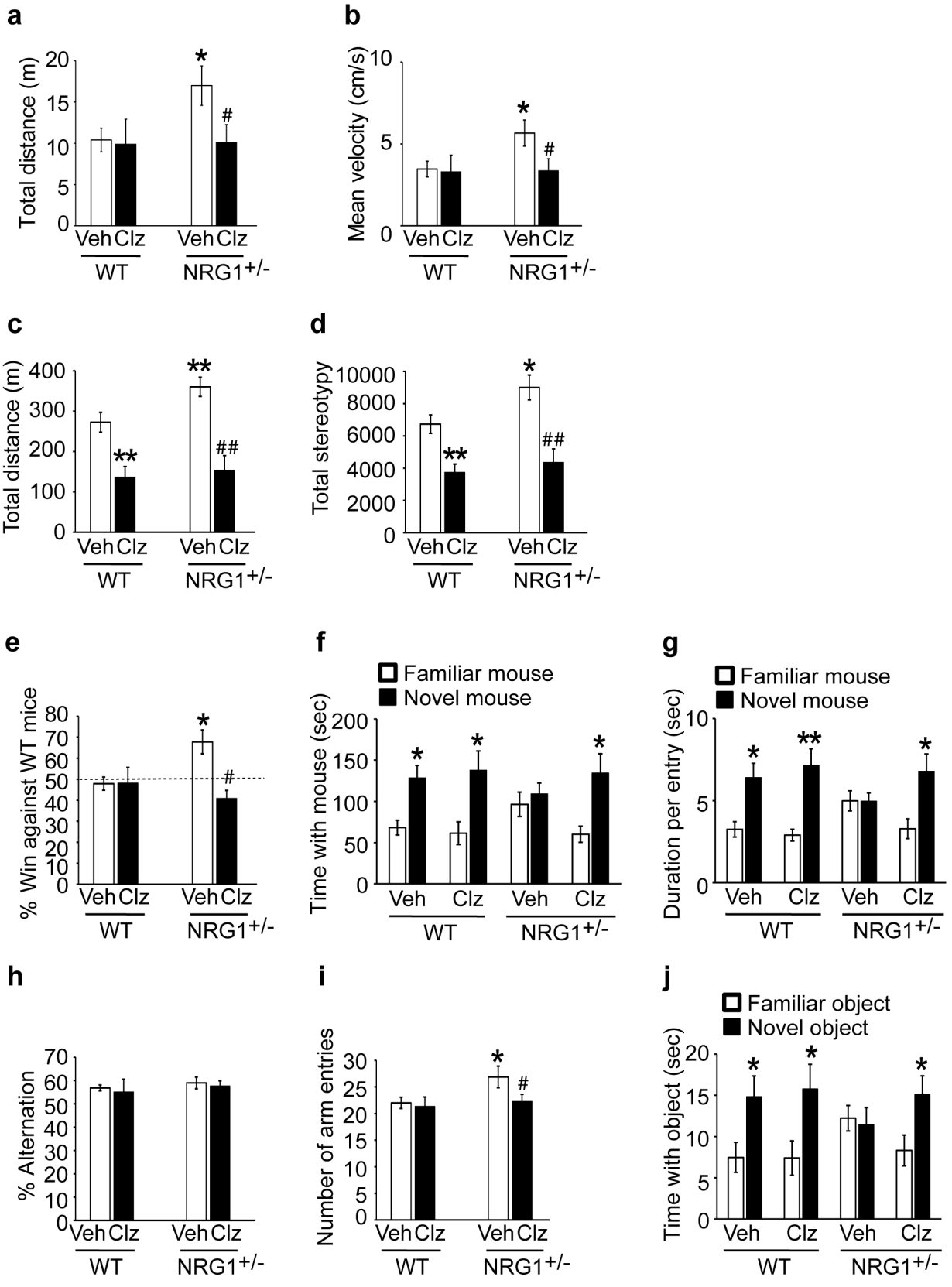
a
Total distance (m)
20
15
10
5
0
*
#
Veh Clz
Veh Clz
WT
NRG1+/-
b
Mean velocity (cm/s)
10
5
0
*
#
Veh Clz
Veh Clz
WT
NRG1+/-
c
Total distance (m)
400
300
200
100
0
**
**
##
Veh Clz
Veh Clz
WT
NRG1+/-
d
Total stereotypy
10000
8000
6000
4000
2000
0
*
**
##
Veh Clz
Veh Clz
WT
NRG1+/-
e
% Win against WT mice
80
70
60
50
40
30
20
10
0
*
#
Veh Clz
Veh Clz
WT
NRG1+/-
f
Familiar mouse
Novel mouse
Time with mouse (sec)
200
150
100
50
0
*
*
*
Veh
Clz
Veh
Clz
WT
NRG1+/-
g
Familiar mouse
Novel mouse
Duration per entry (sec)
10
5
0
*
**
*
Veh
Clz
Veh
Clz
WT
NRG1+/-
h
% Alternation
70
60
50
40
30
20
10
0
Veh Clz
Veh Clz
WT
NRG1+/-
i
Number of arm entries
30
25
20
15
10
5
0
*
#
Veh Clz
Veh Clz
WT
NRG1+/-
j
Familiar object
Novel object
Time with object (sec)
20
15
10
5
0
*
*
*
Veh
Clz
Veh
Clz
WT
NRG1+/-

SI Figure 10. Clozapine reverses behavioral and cognitive deficits in Nrg1$^{+/-}$ mice. Male WT and Nrg1$^{+/-}$ littermates (6-9 months old, 9-16 mice each group) were used for all tests. Vehicle (Veh) or clozapine (Clz, 1 mg/kg, i.p.) was administered 1 h prior to tests. (**a, b**) Clozapine reverses basal hyperactivity in Nrg1$^{+/-}$ mice. Mice were allowed to freely explore in an open-field for 5 min. Total distance (**a**) and mean velocity (**b**) were calculated using ANY-maze. (**c, d**) Clozapine reverses PCP-induced hyperactivity in Nrg1$^{+/-}$ mice. Mice were administered with PCP (7.5 mg/kg, i.p.) for 1 h. Total distance traveled (**c**) and total stereotypic counts (**d**) were recorded and analyzed using Activity Monitor (MED Associates). (**e**) Clozapine reverses aggressive behaviors in social dominance test. Mice were tested in a narrow plastic tube against non-littermate naïve WT mice. Each mouse went through 4 trials and % win was plotted. (**f, g**) Clozapine restores social interaction during social novelty stage in Nrg1$^{+/-}$ mice. During social novelty phase, mice were exposed to a novel non-littermate WT mouse or the familiar mouse. Time spent with each mouse (**f**) and duration per entry (**g**) were analyzed by ANY-maze. (**h, i**) Nrg1$^{+/-}$ mice made more entries in Y-maze, which was reversed by clozapine treatment. Mice were tested in Y-maze for 5 min. Alternation (**h**) and entries to any arm (**i**) were calculated using ANY-maze. (**j**) Clozapine reverses cognitive deficits in Nrg1$^{+/-}$ mice in the novel object recognition (NOR) task. Mice were trained with two identical objects. Twenty-four h post training, mice were tested in the choice phase with one familiar object and one novel object. All data were expressed as mean ± SEM and statistical significance was determined using two-way ANOVA with Bonferroni *post hoc* test for (**a-d, h, i**) or Chi-square one-sample *t*-test against 50% chance for (**e**) or Student *t*-test comparing two objects (**f, g, j**) (*$P < 0.05$, **$P < 0.01$; $^{\#}P < 0.05$, $^{\#\#}P < 0.01$ compared with Nrg1$^{+/-}$ Veh group, n = 9-16 per group).

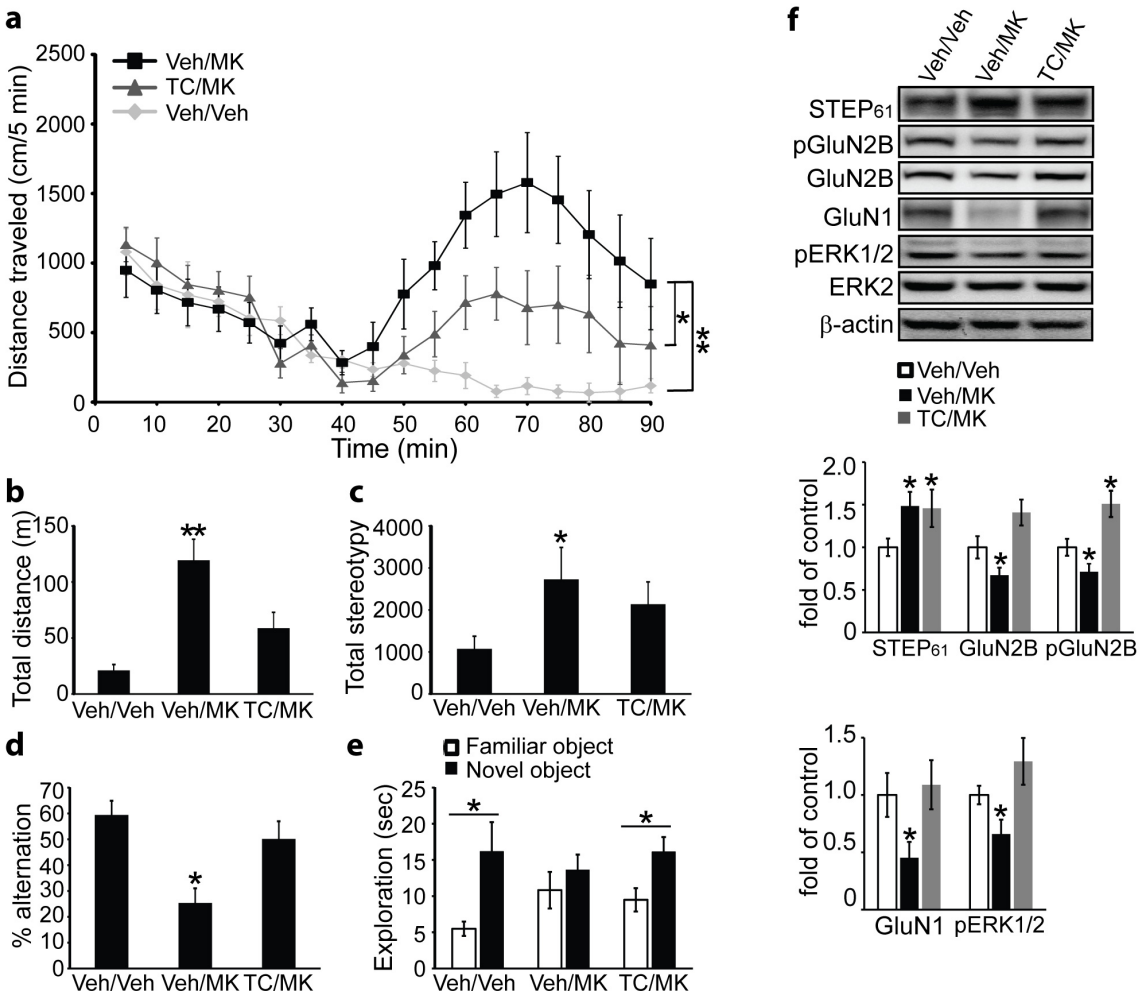

SI Figure 11. STEP inhibitor reverses MK-801-induced motor and cognitive deficits in mice.

Male WT mice (C57BL6/J, 4-6 months old, 8-10 mice each group) were used for all tests. (**a-c**) TC-2153 reverses MK-801-induced hyperactivity in mice. Mice were administered with vehicle (Veh) or TC-2153 (TC, 10 mg/kg, i.p.) 3 h prior to MK-801 (0.15 mg/kg, i.p.) treatment for 1 h. Total distance traveled (**b**) and total stereotypic counts (**c**) were recorded and analyzed using Activity Monitor (MED Associates). (**d**) TC-2153 reverses working memory deficits in the Y-maze task. Mice were tested in Y-maze for 5 min. Spontaneous alternation was calculated using ANY-maze. (**e**) TC-2153 reverses cognitive deficits in the novel object recognition (NOR) task. Mice were trained with two identical objects. Twenty-four h post training, mice were tested in

the choice phase with one familiar object and one novel object. (**f**) TC-2153 restored NMDAR signaling in synaptosomal membrane fraction. P2 fractions were used to probe for STEP and its substrates on WB. All data were expressed as mean ± SEM and statistical significance was determined using two-way ANOVA with repeated measures followed by post hoc Bonferroni test for (**a**) or one-way ANOVA with Bonferroni *post hoc* test for (**b-d, f**) or Student *t*-test comparing two objects (**e**) (**P* < 0.05, ***P* < 0.01 compared with Veh/Veh group, n = 8-10 per group for **a-e**; n = 6 for **f**).

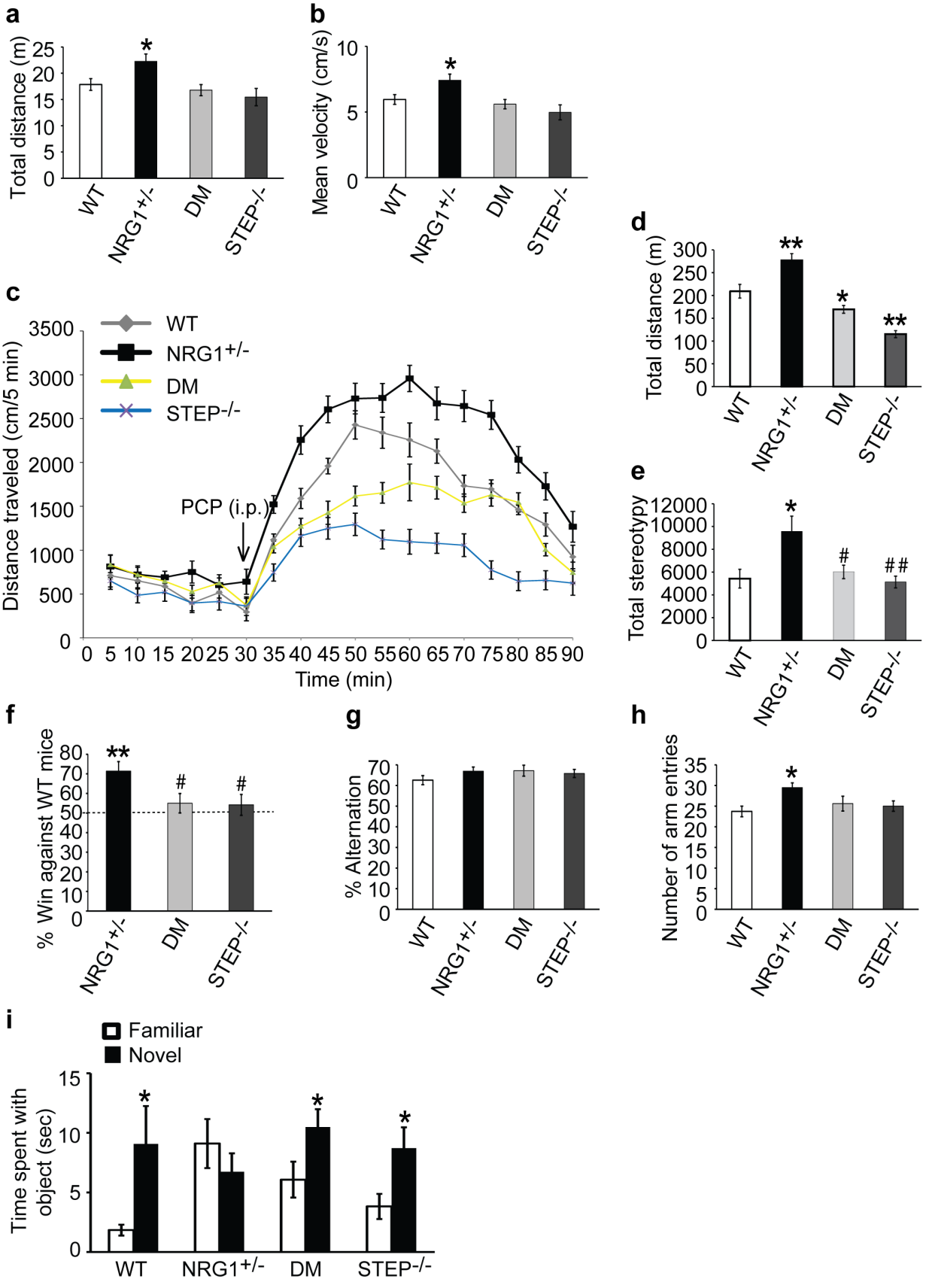
a
Total distance (m)
25
20
15
10
5
0
*
WT
NRG1+/-
DM
STEP-/-
b
Mean velocity (cm/s)
10
5
0
*
WT
NRG1+/-
DM
STEP-/-
c
Distance traveled (cm/5 min)
3500
3000
2500
2000
1500
1000
500
0
WT
NRG1+/-
DM
STEP-/-
PCP (i.p.)
0 5 10 15 20 25 30 35 40 45 50 55 60 65 70 75 80 85 90
Time (min)
d
Total distance (m)
300
250
200
150
100
50
0
**
*
**
WT
NRG1+/-
DM
STEP-/-
e
Total stereotypy
12000
10000
8000
6000
4000
2000
0
*
#
##
WT
NRG1+/-
DM
STEP-/-
f
% Win against WT mice
80
70
60
50
40
30
20
10
0
**
#
#
NRG1+/-
DM
STEP-/-
g
% Alternation
70
60
50
40
30
20
10
0
WT
NRG1+/-
DM
STEP-/-
h
Number of arm entries
35
30
25
20
15
10
5
0
*
WT
NRG1+/-
DM
STEP-/-
i
Familiar
Novel
Time spent with object (sec)
15
10
5
0
*
*
*
WT
NRG1+/-
DM
STEP-/-

SI Figure 12. Genetic reduction of STEP reverses motor and cognitive deficits in Nrg1$^{+/-}$ mice. Male WT, Nrg1$^{+/-}$, Nrg1$^{+/-}$ STEP$^{-/-}$ (double mutant, DM) and STEP$^{-/-}$ littermates (6-9 months old, 9-16 mice each group) were used for all tests. (**a,b**) Genetic reduction of STEP reverses hyperactivity in Nrg1$^{+/-}$ mice. Mice were allowed to freely explore an open-field for 5 min. Total distance (**a**) and mean velocity (**b**) were calculated using ANY-maze. (**c-e**) Genetic reduction of STEP reverses PCP-induced hyperactivity in Nrg1$^{+/-}$ mice. Mice were monitored for basal activities for 30 min, followed by PCP challenge (7.5 mg/kg, i.p.) for 1 h. Distance traveled in each 5 min bin during the 90 min test period (**c**), total distance traveled (**d**) and total stereotypic counts (**e**) were recorded and analyzed using Activity Monitor (MED Associates). (**f**) Genetic reduction of STEP reverses aggressive behaviors in social dominance test. Mice were tested in a narrow plastic tube against non-littermate naïve WT mice. Each mouse went through 4 trials and % win was plotted. (**g, h**) Nrg1$^{+/-}$ mice made more entries in Y-maze, which was reversed by genetic reduction of STEP in DM mice. Mice were tested in Y-maze for 5 min. Alternation and entries to any arm were calculated using ANY-maze. (**i**) Genetic reduction of STEP reverses cognitive deficits in Nrg1$^{+/-}$ mice in the novel object recognition (NOR) task. Mice were trained with two identical objects. Twenty-four h post training; mice were tested in the choice phase with one familiar object and one novel object. All data were expressed as mean ± SEM and statistical significance was determined using two-way ANOVA with repeated measures followed by Bonferroni *post hoc* test for (**c**) or one-way ANOVA with Bonferroni *post hoc* test for (**a, b, d, e, g, h**) or Chi-square one-sample *t*-test against 50% chance for (**f**) or Student *t*-test comparing two objects (**i**) (*$P < 0.05$, **$P < 0.01$; $^{\#}P < 0.05$, $^{\#}P < 0.05$ compared with Nrg1$^{+/-}$ group, n = 9-16 per group).

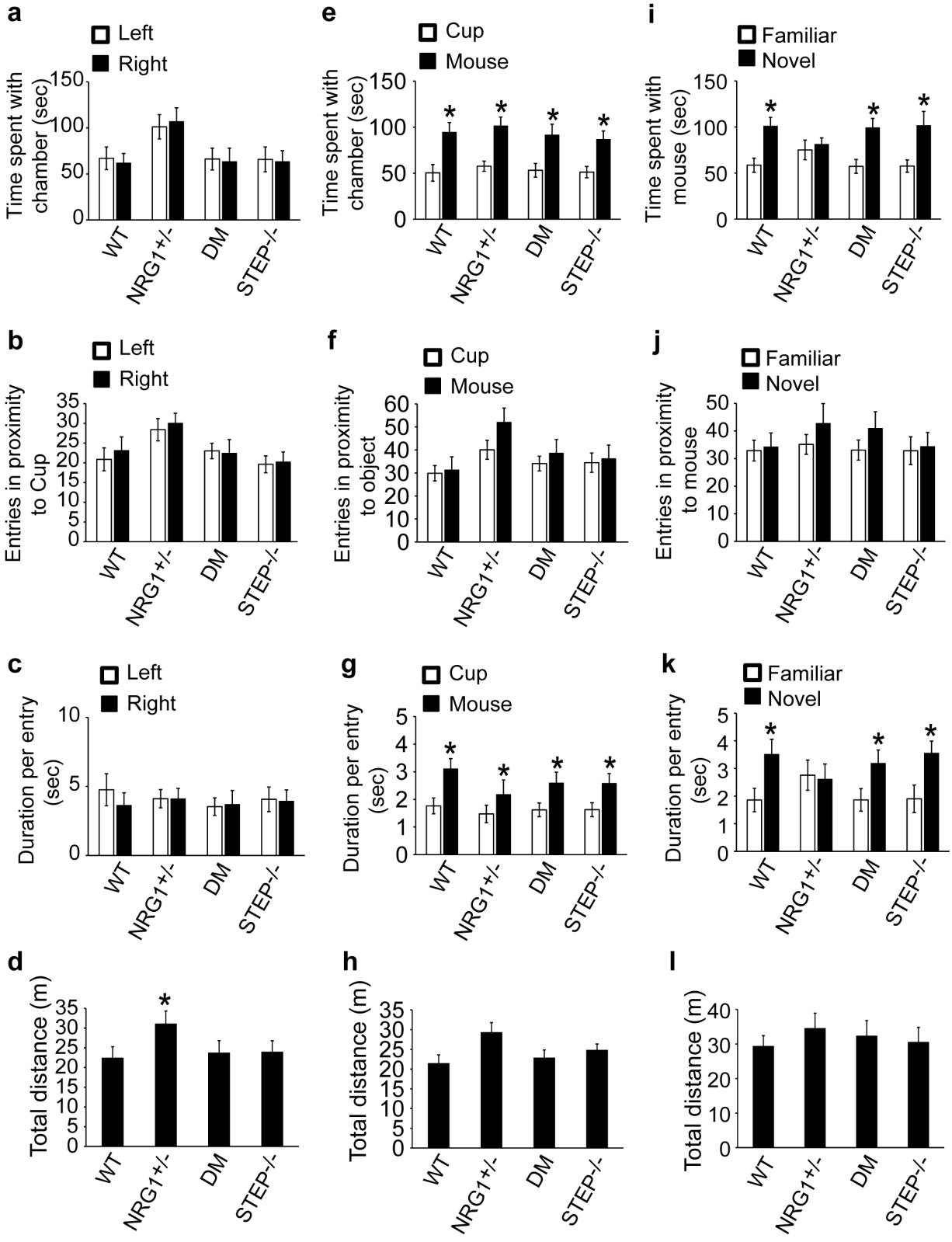
a
Left
Right
Time spent with chamber (sec)
150
100
50
0
WT
NRG1+/-
DM
STEP-/-
e
Cup
Mouse
Time spent with chamber (sec)
i
Familiar
Novel
Time spent with mouse (sec)
b
Entries in proximity to Cup
35
30
25
20
15
10
5
0
f
Entries in proximity to object
60
50
40
30
20
10
0
j
Entries in proximity to mouse
50
40
30
20
10
0
c
Duration per entry (sec)
10
5
0
g
5
4
3
2
1
0
k
d
Total distance (m)
35
30
25
20
15
10
5
0
h
l
40
30
20
10
0

SI Figure 13. Genetic reduction of STEP reverses social deficits in Nrg1$^{+/-}$ mice. Male WT, Nrg1$^{+/-}$, Nrg1$^{+/-}$ STEP$^{-/-}$ (double mutant, DM) and STEP$^{-/-}$ littermates (6-9 months old, 9-16 mice each group) were used for all tests. Three-chamber social task was used to access social interactions during habituation (**a-d**), social preference (**e-h**) and social novelty (**i-l**). (**a-d**) Nrg1$^{+/-}$ mice did not show deficits during habituation of 3-chamber social interaction. Mice were placed in the center chamber and allowed to explore all three chambers for 10 min. Two empty cups were kept in the left and right chambers. (**e-h**) Nrg1$^{+/-}$ mice did not show deficits in social novelty. After habituation, mice were placed in the center chamber, with one empty cup and one strange mouse in the left and right chambers. Mice were allowed to explore all three chambers for 10 min. Close proximity within 1 inch around the cup that has the strange mouse under it was considered as social interaction. Social behaviors were recorded using ANY-maze. (**i-l**) Genetic reduction of STEP restores social interaction during social novelty stage in Nrg1$^{+/-}$ mice. Mice were tested in the third 10-min session for preference for a novel non-littermate mouse versus the familiar mouse. All data were expressed as mean ± SEM and statistical significance was determined using one-way ANOVA with Bonferroni *post hoc* test for (**d, h, l**) or Student *t*-test comparing two objects (**a-c, e-g, i-k**) (**P* < 0.05, n = 9-16 per group).

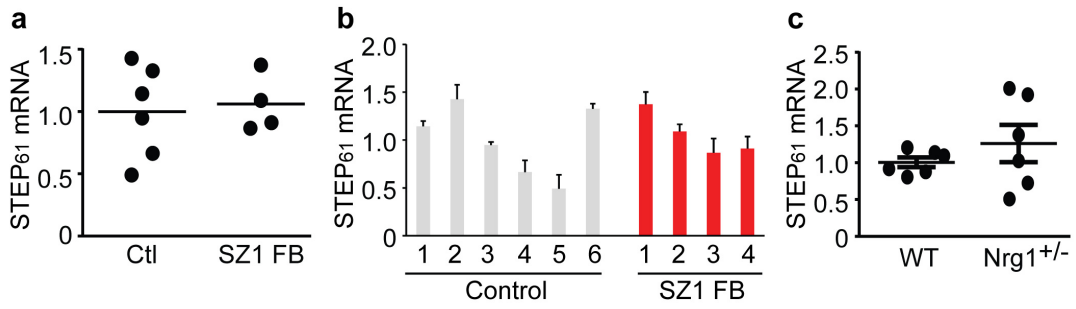

SI Figure 14. $STEP_{61}$ mRNA levels do not change in SZ1-FB hiPSC neurons or $Nrg1^{+/-}$ mice. RT-PCR comparison of basal levels of $STEP_{61}$ mRNA (*PTPN5*) (relative to *GAPDH*). (**a, b**): No differences in basal levels of $STEP_{61}$ mRNA (*PTPN5*) in SZ1-FB hiPSC neurons (by group average (**a**) or by individual (**b**)). (**c**): No differences in basal levels of $STEP_{61}$ mRNA (*PTPN5*) in brain of $Nrg1^{+/-}$ mice.

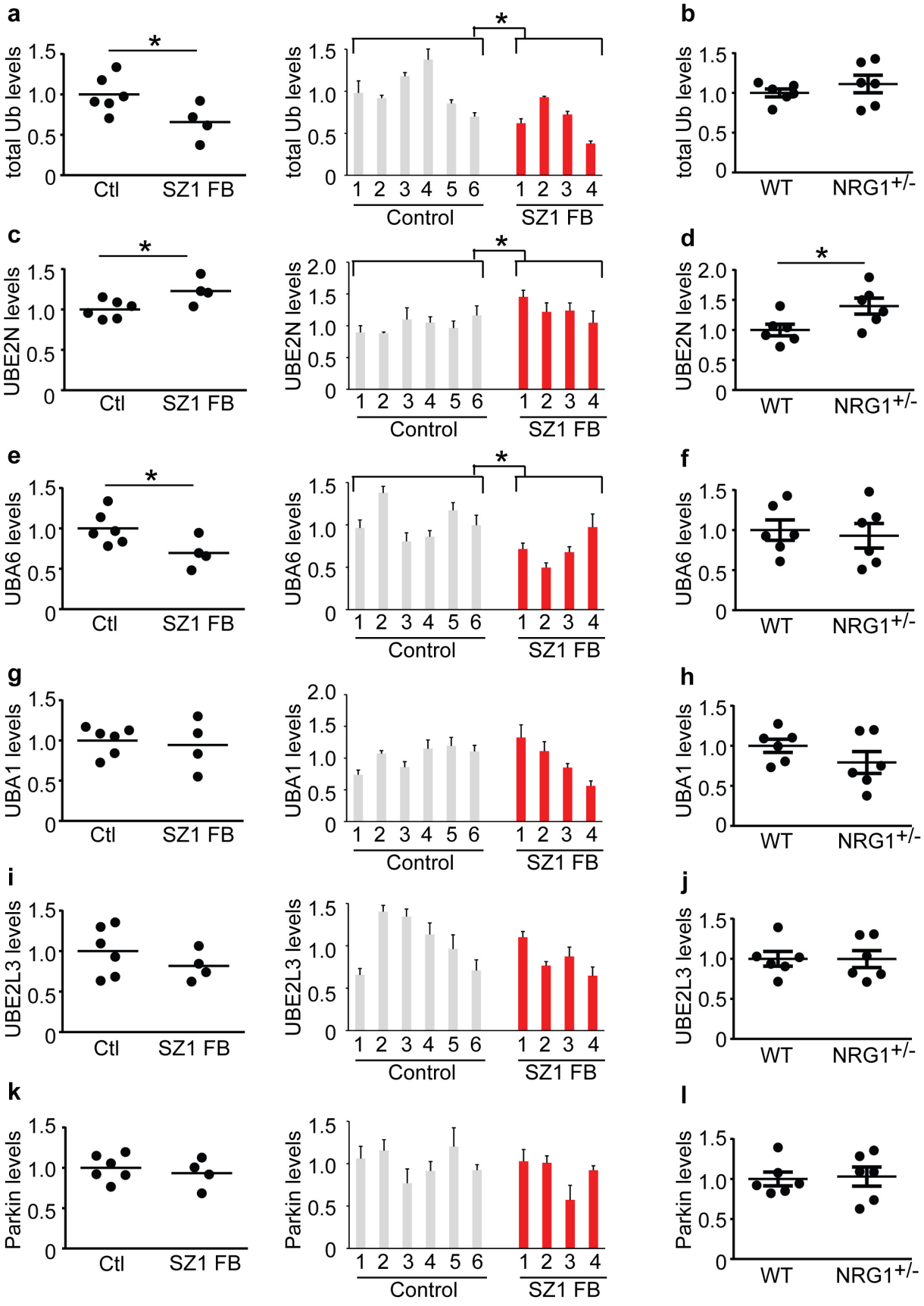
a
total Ub levels
Ctl
SZ1 FB
Control
b
WT
NRG1+/-
c
UBE2N levels
d
e
UBA6 levels
f
g
UBA1 levels
h
i
UBE2L3 levels
j
k
Parkin levels
l

SI Figure 15. Dysregulation of UPS components in SZ1-FB hiPSC neurons or Nrg1$^{+/-}$ mice. **a, c, e, g, i and k**: control and SZ1-FB hiPSC neurons (by group average (left) or by individual (right)); **b, d, f, h, j and l**: male wild type and Nrg1$^{+/-}$ mice. (**a, b**) Affinity purification of ubiquitinated proteins using TUBE revealed a significant decrease in SZ1-FB forebrain neurons (**a**) but no change in Nrg1$^{+/-}$ mice (**b**). (**c, d**) Western blot for E2 conjugating enzyme UBE2N detected increased levels in both SZ1-FB hiPSC neurons (**c**) and Nrg1$^{+/-}$ mice (**d**). (**e, f**) Western blot for E1 activating enzyme UBA6 detected decreased levels in SZ1-FB hiPSC neurons but no change in Nrg1$^{+/-}$ mice. (**g-l**) Western blot for ubiquitin E1 activating enzyme UBA1 (**g, h**), ubiquitin E2 conjugating enzyme UBE2L (**i, j**) and ubiquitin E3 ligase Parkin (**k, l**) revealed no changes in total protein levels in either SZ1-FB hiPSC neurons or Nrg1$^{+/-}$ mice. All data were expressed as mean ± SEM and statistical significance was determined by JMP nested analysis using standard least squares analysis, followed by Student *t*-test for **a, c, e, g, i and k** or Student *t*-test **b, d, f, h, j and l** (*$P < 0.05$, n = 3-6 biological replicates for SZ1-FB hiPSC neurons; n = 6 per group for mice).

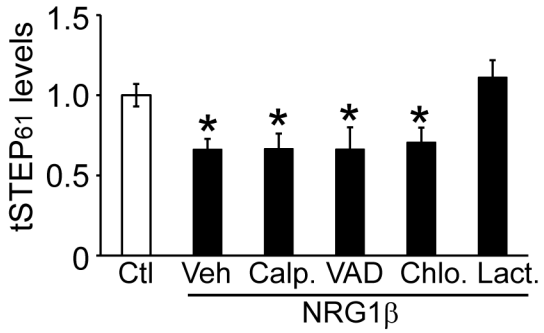

SI Figure 16. NRG1 signaling leads to proteasome-dependent degradation of $STEP_{61}$. Rat cortical neurons were pretreated with vehicle (0.1% DMSO) or inhibitors for calpain (calpeptin, 10 μM), caspase (cpo-VAD-CHO, 10 μM), lysozyme (chloroquine, 500 μM) or the proteasome (lactacystin, 5 μM), followed by NRG1β treatment (10 nM, 30 min). Total $STEP_{61}$ levels were normalized to β-actin as a loading control. All data were expressed as mean ± SEM and statistical significance was determined by one-way ANOVA with Bonferroni *post hoc* test (*$P < 0.05$, n = 6 per group).